Fate of polycyclic aromatic compounds from diluted bitumen spilled into freshwater limnocorrals

Stoyanovich, S[a]., Yang, Z[b]., Hanson, M[d]., Hollebone, B.P[b]., Orihel, D. M[c]., Palace, V[e]., Rodriguez-Gil, JR[a,e]., Mirnaghi, F[b]., Shah, K[b]., Blais, J.M[a*]

[a] Department of Biology, University of Ottawa, Ottawa, Ontario, K1N 6N5, Canada

[b] Emergencies Science and Technology Section, Environment and Climate Change Canada, Ottawa, Ontario, Canada

[c] Department of Biology and School of Environmental Studies, Queen's University, Kingston, ON K7L 3N6

[d] Department of Environment and Geography, University of Manitoba, Winnipeg, MB, R3T 2N2, Canada.

[e] International Institute for Sustainable Development, Experimental Lakes Area, 111 Lombard Avenue, Suite 325, Winnipeg, Manitoba R3N 0T4, Canada

Corresponding authors: Dr. Sawyer S. Stoyanovich
University of Ottawa
75 Laurier Ave E
K1N 6N5, Ottawa, ON, Canada
Tel: +1 (613) 323-3279
Email: sstoy012@uottawa.ca

Abstract

Diluted bitumens (dilbits) are produced by mixing highly viscous bitumen with lighter petroleum products to facilitate transport. The unique physical and chemical properties of dilbit may affect the environmental fate and effects of dilbit-derived chemical compounds when spilled. To further explore this, we monitored experimental spills of Cold Lake Winter Blend (CLWB) dilbit for 70 days in limnocorrals installed in a freshwater boreal lake. A regression design with 2 controls and 7 treatments was used to assess the fate and behaviour of polycyclic aromatic compounds (PACs) as they partitioned from the dilbit into the air, water column and sediments. Treatments ranged from 1.5 to 180 L of CLWB, resulting in oil:water ratios ranging between 1:71 000 to 1:500 (v:v). We began to detect elevated concentrations of PACs as early as 6 hrs post-addition in the air, 12 hrs post-addition in the water column, and 15 – 28 d post-addition in the sediments. By the end of the experiment, concentrations of PACs had largely declined in the water column but remained elevated in the sediments. Our results demonstrate that under conditions typical of temperate boreal lakes, only a small proportion of PACs from dilbit enters the aquatic system, but even so, may produce concentrations of ecotoxicological concern, especially in the sediments, which is the ultimate sink for dilbit-derived PACs.

Keywords

Dilbit; Natural weathering; Limnocorral; Polycyclic aromatic compounds; Freshwater

1.0 Introduction

The Alberta oil sands make up one of the largest petroleum deposits on Earth, with estimated reserves of 170 billion barrels of bitumen (CAPP, 2019; Lee et al., 2015). Bitumen is a highly viscous form of crude oil that must be diluted with natural gas condensates to facilitate pipeline transport, forming diluted bitumen or dilbit (Crosby et al., 2013; Fingas, 2015). Despite environmental concerns and proposed pipeline expansions, little is known about the environmental fate and effects of dilbit spills, especially in freshwater areas such as inland lakes (Crosby et al., 2013; Fitzpatrick et al., 2015; Lee et al., 2015; NASEM, 2016; Yang et al., 2020). Oil spills to freshwater can pose major threats to the receiving environment by compromising water supplies and affecting areas of dense human population (Owens et al., 1993). Inland lakes also have limited dispersion and dilution capabilities compared to ocean systems, although oil spills in freshwater are typically much smaller than in ocean settings (Lee et al., 2015). In an open sea system, breaking waves and tidal action can facilitate the transport and dissipation of oil spills, but in low-energy freshwater environments such as sheltered lakes, oil is retained for longer periods of time (Baca and Getter, 1985) with potential to pose long term risk.

While marine spills often receive more attention due to higher volumes of petroleum spilled and far reaching economic damage, a number of large scale freshwater spills have also occurred. In 2005, a train derailment caused a 149,500 L spill of Bunker C heavy fuel into Wabamun Lake, Alberta, Canada (Debruyn et al., 2007). In 2010, a pipeline rupture led to the release of 3.2 million L of Cold Lake Blend (CLB) dilbit into Talmadge Creek, and eventually the Kalamazoo River in Marshall,

Michigan (US EPA, 2013). In 2013, a pipeline carrying Wabasca heavy crude oil ruptured in Mayflower, Arkansas, releasing approximately 795,000 L of oil into a residential neighborhood that eventually drained into Lake Conway (Kennon and Bouldin, 2015). In 2016, the rupture of a Husky Energy pipeline in Lloydminster, Saskatchewan released approximately 225,000 L of diluted heavy crude oil, 40% of which entered the North Saskatchewan River (Husky Energy Inc, 2016; Yang et al., 2020). While such accidental spills provide an opportunity for researchers to study impacts of a dilbit spill in freshwater environments, they have their limitations. Because physical recovery of the spilled oil is top priority, environmental sampling is often delayed or influenced by clean-up activities. Such studies are also hampered by the unexpected nature of a spill; it is difficult to plan a proper study around an accidental spill that occurs without warning.

Following the early stages of an oil spill in an aqueous system, volatile and slightly water-soluble compounds will partition to the air and water column (Lee et al., 2015), leaving behind a recalcitrant oil residue (Tarr et al., 2016). Of these slightly water-soluble compounds, oil-derived polycyclic aromatic compounds (PACs) have garnered much attention in the scientific literature due to their toxicity, carcinogenicity and relative resistance to biodegradation (specific to the larger 3-5 ringed PACs) (Achten and Andersson, 2015; Lee et al., 2015; Van Hamme et al., 2003). Therefore, PAC concentrations in the water column following a spill can provide estimates of the potential for toxicity (Neff and Stubblefield, 1995; Reddy and Quinn, 2001). Studies have shown that the dissolution of hydrocarbon occurs within the initial hours following a spill (Brussaard et al., 2016; Gros et al., 2014; Ortmann et al., 2020; Stoyanovich et al.,

101 2019). While dissolution only accounts for a very small portion of the total oil loss
102 (Fingas, 2015; Lee et al., 2015), dissolution can still result in the exposure of aquatic
103 biota to potentially toxic compounds. Contamination can also extend down to the
104 sediments, where hydrophobic compounds may bind to suspended and/or sinking
105 sediment and persist over long periods of time (Lee et al., 2003). The weathered oil-
106 residue is enriched in recalcitrant hydrocarbons, of which petroleum biomarkers are a
107 notable example. Biomarkers consist of a group of cyclic alkanes (i.e. hopanes,
108 steranes, and terpanes) that are resistant to environmental degradation and are thus
109 used in the field of environmental forensics as markers of petroleum contamination
110 (King et al., 2014; Lee et al., 2015; Venosa et al., 1997). Characterizing the
111 environmental fate of these chemical constituents in crude oil under realistic conditions
112 is therefore crucial to understanding the fate of dilbit and the potential ecotoxicological
113 effects of spills in aquatic systems (Bejarano et al., 2014).
114 This work focuses on describing the quantity and distribution of aromatic
115 compounds in the water columns and sediments of the limnocorrals following the spills.
116 Here, we report results from a series of seven controlled dilbit spills (with two controls),
117 ranging in dilbit volume from 1.5 to 180 L, into limnocorrals installed in a small boreal
118 lake located in Northwestern Ontario, Canada. Our experimental design is unique in that
119 we simultaneously collected air, water column and sediment samples immediately
120 following the spills (6 h post-spill) and 12 times over a period of 70 days. This time
121 series enables us to describe both the short- and long-term behaviour of the oil-derived
122 compounds as they partition from the surface oil slick to the air, water, and sediments of

123 the limnocorrals. This study will improve models of hydrocarbon partitioning in the
124 environment immediately following a dilbit spill into a boreal lake.
125
126 **2.0 Methods**
127 *2.1 Experimental Spills and Sampling*
128 The experiment consisted of nine in-lake limnocorrals deployed along the
129 northwestern littoral zone of Lake 260 at the International Institute for Sustainable
130 Development Experimental Lakes Area (IISD-ELA) in Kenora, Ontario, Canada. The
131 limnocorrals were 10 m in diameter and consisted of a floating ring to which we
132 attached a high-density polyethylene (HDPE) cylindrical membrane that extended to the
133 sediments at a depth ranging from 1.5 – 2 m (SI Figure S1). We used two layers of
134 sandbags around the perimeter to seal the plastic membrane onto the lake bottom (SI
135 Figure S2). The experimental set-up has been previously described in detail
136 (Rodriguez-Gil et al., 2021). On June 20th, 2018, we pumped Cold Lake Winter Blend
137 dilbit (CLWB) onto the water surface of the treatment limnocorrals. The logistical
138 considerations of the CLWB additions have been described by Shah et al. (2019). The
139 addition of water containing a known amount of tritium (^{3}H) to each limnocorral at the
140 beginning of the experiment, as described in detail by Rodríguez-Gil et al. (2021),
141 allowed us to accurately determine the water volume inside the limnocorrals and
142 characterize any potential water exchange through leaks or ruptures with the lake.
143 Limnocorral water volumes ranged from 90.7 to 106.5 m^3. No visible gaps, ruptures, or
144 holes were observed in any of the limnocorrals.

145 Seven limnocorrals each received a different volume of CLWB: (1.5, 2.9, 5.5, 18,
146 42, 82, and 180 L), and two limnocorrals did not receive any dilbit (one near-field
147 control, NFC and one far-field control, FFC) (SI Figure S3). The range in spill volumes
148 resulted in oil:water ratios within the limnocorrals ranging from 1:71 000 to 1:500 v/v.
149 We selected these oil:water ratios based on published onshore crude oil spill
150 occurrences throughout North America between 2008 and 2017 (NEB, 2017; USDOT,
151 2017). The lower limit of 1.5 L replicates the most common onshore spill size, while the
152 upper limit of 180 L produces an oil:water ratio similar to that of the largest inland spill to
153 date, the 2010 Kalamazoo River spill. A detailed rationale for our spill volume selection
154 was published elsewhere (Rodriguez-Gil et al., 2021).
155 These experimental spills lasted a total of 70 days, throughout which we
156 collected air, water, and sediment samples to assess how these environmental
157 compartments change over time following the introduction of dilbit (Figure 1).
158
159 *2.2 Water Column Sampling*
160 We collected water samples for hydrocarbon analysis from the center of each
161 limnocorral at two depths (0.1 m and 1.5 m) below the water surface at -1, 0.25, 1, 2, 4,
162 8, 15, 22, 28, 42, 56 and 70 days following the dilbit additions (Figure 1). The water was
163 pumped from the center-point of each limnocorral through 0.6 cm inner diameter high
164 density polyethylene (HDPE) tubing connected to a Spectra Field-Pro Peristaltic Pump
165 (flow rate of 1 L min^{-1}) located on the adjacent dock (SI Figure S1). The first 1 L of each
166 sample was discarded, after which approximately 1 L of water was collected into pre-
167 weighed, certified-clean amber glass bottles with Teflon film cap liners filled to the top to

minimize headspace and any evaporation of volatile compounds. The collected water samples are representative of bulk (unfiltered) samples that include both dispersed and dissolved oil components. There are currently no accepted methods for separating dispersed oil droplets from the dissolved phase in water samples and attempts to do so reduce the realistic nature of field samples (Lee et al., 2015). Preliminary analysis of the total petroleum hydrocarbon (TPH) and total polycyclic aromatic compound (TPAC) concentrations of these samples indicated no significant differences between the top and bottom water column measurements in any of the treatments, indicating vertical mixing in the water column (Rodriguez-Gil et al., 2021). Because of this, the results from top and bottom measurements were averaged to simplify analyses.

Due to rigorous sampling schedules and intensive analytical demands, only four of the seven treatments: NFC, 1.5 L, 18 L, and 180 L, were chosen to be sampled in triplicate at each depth and timepoint, while single samples were collected from all other treatments.

2.3 Sediment Sampling

Due to the large surface area of the limnocorrals (approx. 75 m^2) and the inability to enter the limnocorrals by boat once the experiment had commenced, all sediment sampling had to be done from the adjacent docks. Invasive techniques such as Ponar dredging, coring, or Ekman grab sampling could not be used as they would significantly disturb the sediment bottom and re-suspend sediment particles that can in turn alter the fate of the dilbit. Therefore, prior to the beginning of the experiment, a series of 250 mL pre-cleaned glass jars were filled with sediments collected from each limnocorral plot

and then placed on the sediment bottom directly below the oil-free partition area (SI Figure S1). At each timepoint after the spills, a single jar from each treatment was pulled up through the partition at -3, 1, 2, 8, 15, 22, 28, 42- and 70-days following dilbit addition (Figure 1). Due to the placement of these jars below the oil-free partition, no sediment samples showed signs of physical oiling during the study. At the end of the experiment and prior to decommissioning, we entered both the 18 and 82 L treatments and collected 3 sediment cores from both treatments near the centre-point of the limnocorral. We chose areas to core where the sediments were visibly oiled with tarballs, that is, visible discrete spherical agglomerations of oil and sediment ranging in diameter between 5-10 cm. We then collected the sediment cores with the tarballs centered in the coring tube (SI Figure S4), removed the tarball and collected the top 3 – 5 cm of the sediment core for PAC analysis. This enabled us estimate the level of sediment contamination following dilbit submergence events.

2.4 Air Sampling

We conducted air monitoring in the 180 L, 18 L, and NFC during the first 8 days of the study only as we assumed further evaporation would be neglible after 8 days. We collected air samples 0.3 m above the water's surface and roughly 1 m from the northern edge of the limnocorrals (SI Figure S1). Air samples were collected at 0-, 0.25-, 1-, 2-, 4-, and 8-days post dilbit release from each of the three limnocorrals. At each sampling timepoint, we ran air samplers for a 60-minute period at a flow rate of 5 L min^{-1}. The air samplers consisted of a GilAir® Plus Air Sampling Pump (Levitt Safety, Ottawa, ON), connected to a sampling cartridge via polyvinyl chloride (PVC) connecting

tube (Fisher Scientific, Ottawa, ON, Canada). The cartridge contained polyurethane foam (PUF) (URG Corporation, Chapel Hill, NC) and a Quartz filter (25 mm) (Whatman, Maidstone, UK). The pumps were calibrated before sampling using a Gilian Gilibrator-2 Calibrator (Levitt Safety, Ottawa, ON). All Quartz filters were baked at 400°C for 5 h prior to use. Following sample collection, the PUFs and filters were stored in pre-baked aluminum foil and stored in a freezer.

2.5 Sample Analyses

Three separate subsamples of the fresh source CLWB were collected, weighed, and diluted with hexane to an appropriation concentration for further fractionation and chemical analysis. Appropirate amounts of the CLWB solution were spiked with a certified standard mix of surrogates (o-terphenyl, d_{50}-tetracosane, d_8-naphthalene, d_{10}-acenaphthene, d_{10}-phenanthrene, d_{12}-benz[a]anthracene, and d_{12}-perylene) and fractionated through a preconditioned chromatographic column packed with 3 g of silica gel. We performed fractionation and instrumental analysis following the same procedure as Yang et al. (2017) to produce concentrations of each individual analyte included in SI Table S1.

All water samples were processed and extracted for a total of 46 PACs and 21 petroleum biomarkers (SI Table S1) on the same day of collection. Samples were spiked with the same surrogates mentioned above, extracted with 50 mL of dichloromethane (DCM) for 16 hours on a continuous roller apparatus, and then fractionated into different fractions for further analysis. Triplicate lab blanks were run

236 with ultra-pure Milli-Q water and all PAC concentrations were blank-corrected. The
237 sample and instrumental analysis followed the procedures of Yang et al. (2018).
238 The top 3 – 5 cm of sediment in each jar and core sample was removed,
239 homogenized and dried with sodium sulphate, spiked with the same surrogates
240 previously mentioned above, and then Soxhlet extracted with DCM for at least 16 hours.
241 Both sediment jar and core samples were stored, processed, and analyzed using the
242 exact same methods. The extracts were then treated in the same manner as the water
243 samples mentioned above. A total of 46 PACs were analyzed for fresh source oil,
244 sediment and water samples in this work.
245 For air samples, prior to extraction, PUFs and filters, spiked with the same
246 surrogate mix outlined above. PUFs and filters, were extracted using Accelerated
247 Solvent Extraction (ASE 200, Dionex Corporation, Sunnyvale, CA, USA). Following
248 extraction, samples were fractionated by a silica gel chromatographic column with a 1:1
249 mixture of dichloromethane (DCM) and hexane to produce an aromatic fraction (PACs).
250 Samples were then spiked with an internal standard, *p*-terphenyl-d_{14} (Cambridge
251 Isotope Laboratories, Tewksbury, MA 01876) at 1000 pg/L, vortexed, and refrigerated
252 until instrumental analysis. A total of 40 PACs (SI Table S1) were quantified by gas
253 chromatography coupled with mass spectrometry (GC-MS) for all air samples. All
254 samples were blank corrected to remove background PAC contamination and recovery
255 corrected.
256 Percent recoveries of surrogates ranged from 71 – 92 % for water samples, 74 –
257 104 % for sediment samples, 87 – 103% for fresh source oil, and 52 – 97 % for air
258 samples (SI Table S2).

2.6 Data Modelling and Analyses

We used R Studio version 1.1.383 (RStudio., Boston, MA, USA) to perform all statistical analyses and graphical representations. We employed a similar approach to Rodriguez-Gil et al. (2021) to facilitate the analysis of treatment effects. Briefly, a simple linear regression was utilized to assess oil:water ratio as a predictor for PAC contamination in the water column and sediments by regressing the concentration against the nominal oil:water ratio at each sampling timepoint. For this purpose, only data collected from dilbit-treated limnocorrals were included in regression analyses, while all data from controls were omitted. Since the dilbit treatments were evenly spaced from one another on a logarithmic scale, oil volumes were $\log_{10}$-transformed prior to analysis to satisfy assumptions of normality. We also used principal component analysis (PCA) to explore similarities and differences between environmental water and sediment samples and the spilled CLWB dilbit reflected in their chemical profiles, similar to the work by Allan et al. (2012).

3.0 Results and Discussion

3.1 Hydrocarbon Contamination of the Water Column

The temporal progression of water column PACs in each treatment can be characterized by an initial increase phase, a brief plateau at the maxima, and a subsequent decrease phase (Figure 2). The most abundant PAC families were the naphthalenes ($\Sigma NAP_{C0\text{-}C4}$) in all treatments except for 2.9 and 1.5 L, where phenanthrenes ($\Sigma PHEN_{C0\text{-}C4}$) and dibenzothiophenes ($\Sigma DBT_{C0\text{-}C3}$) were the most

abundant PAC families, respectively. Maximum concentrations of these repecteive PAC families in the oil-treated limnocorrals occurred on day 22 for the 180 and 82 L, day 15 for the 42 and 18 L, day 2 in the 5.5 L, and day 8 in the 2.9 and 1.5 L. Compositional patterns of alkylated PAC families in water samples indicate the dominant PACs were the naphthalenes ($\Sigma NAP_{C0\text{-}C4}$), phenanthrenes ($\Sigma PHEN_{C0\text{-}C4}$), fluorenes ($\Sigma FLU_{C0\text{-}C3}$), and dibenzothiophenes ($\Sigma DBT_{C0\text{-}C3}$), together accounting for 16– 54%, 14 – 26%, 14 – 31%, and 14 – 32% of maximum total PAC, denoted as ΣPAC_{46} (Rodriguez-Gil et al., 2021), concentrations across all treatments (SI Figure S5B).

Notably, we found an uncharacteristic spike of $\Sigma NAP_{C0\text{-}C4}$ between days 1 and 2 in each oil treatment which was not observed in the controls (Figure 2). These results may have arisen from cross-contamination of water samples with the dilbit slicks during sampling, analytical error, field sampling variability, or contamination from boats during sampling. Since we are unable to determine the source of this inconsistency, and it is possible that these results do reflect the true nature of the experiment, we chose to include them in all analyses.

Water samples in all dilbit treatments were typically dominated by C1, C2, and C3 alkylated homologs compared to parent compounds (SI Figure S6), likely reflecting the relatively low concentrations of parent PACs (4.9 – 68 ug/g) in the source dilbit (SI Figure S7). While accumulation of PACs in the water column was dominated by 2 – 3 ring compounds, their concentrations were not significantly related to log K_{OW} (SI Figure S8). The most abundant PAC group in the 180, 42, 18, 5.5, and 2.9 L limnocorrals was the C_4-NAPs, reaching concentrations of 509 ± 25, 317 ± 10, 150 ± 17, 189 ± 33, and 74 ± 6 ng/L, respectively. The C_3-NAP homologues were the most abundant group in

the 82 L treatment (323 ± 7 ng/L), and C_2-DBT group, the most abundant in the 1.5 L treatment (160 ± 17 ng/L) (SI Figure S6), similar to our previous tank study (Stoyanovich et al., 2019). Tritium profiles of the 18 and 82 L treatments suggested water exchange with the lake (at rates of 0.035 and 0.016 d^{-1}, respectively), which were an order of magnitude greater than the leakage rates of the remaining treatments (Rodriguez-Gil et al., 2021); therefore, PAC concentrations in the 18 and 82 L treatments were likely underestimated. The concentrations in the 18 and 82 L treatments thus reflect what would occur following a dilbit spill in an enclosed or semi-enclosed boreal lake, where water exchange is low. In large open systems such as coastal environments or large lake systems such as the Great Lakes, water exchange in and out would result in rapid decreases in water column PACs by dilution (Ortmann et al., 2020). It is also important to note that PAC water column concentrations observed in these limnocorrals are likely overestimating what would be experienced in natural lake systems with constant inflow and outflow, which can play an important role in dilution.

There are several possible explanations for the observed decline in water-borne PAC concentrations (Figure 2). First, the thick, highly weathered crust that formed on the exterior of the dilbit slicks early on in experiment (Stoyanovich et al., 2021) may have limited further dissolution as time progressed. This crust is thought to be formed following the loss of low molecular weight compounds (Fingas, 2015), leaving behind heavy resins and asphaltenes that migrate to the oil-water interface during emulsification (Fingas and Fieldhouse, 2009), and decrease dissolution rates (Fingas, 2015). Second, the retreating dilbit-slick cover would increase the surface area of open water inside the limnocorrals. This increase in open water over the course of the

328 experiment would facilitate PAC evaporation across the air – water interface. Initially,
329 the dilbit spread to cover the majority (15 – 100%) of the water's surface (Saunders et
330 al., In Prep), however with wind action, gaps formed in the slicks and created sections
331 of open water, adding to the oil slick weathering effects. Open water became even more
332 apparent as the slicks began to sink on day 12 in the lowest-volume oil treatment and
333 day 31 in the highest-volume oil treatment (Saunders et al., In Prep; Stoyanovich et al.,
334 2021). Surface slicks would act as a barrier to evaporation (King et al., 2019), thus as
335 this barrier is removed, PAC evaporation from the water column would accelerate.
336 Saunders et al. (In Prep) tracked the evaporation of a volatile tracer gas, sulfure
337 hexafluoride (SF_6), in these same limnocorrals. The authors found that SF_6 evaporation
338 rates decreased by up to 80% with increasing dilbit slick cover due to the reduction of
339 open-water area where chemical exchange across the air-water interface could occur.
340 This corroborates our observations in the 180 L treatment, where the surface dilbit slick
341 remained for a longer period of time (31 d) compared to the other treatments
342 (Stoyanovich et al., 2021) (12 – 22 d), resulting in a slower PAC depletion in the water
343 column (Figure 2A). Third, PACs in the water column partitioned to the sediments,
344 reflective of their preference for the organic phase (discussed in section 3.3). Likely, a
345 combination of these processes resulted in the observed depletion of PACs in the water
346 column of the limnocorrals.
347 Drawing comparisons between our results and those of other studies is
348 challenging as factors such as experimental setting, dilbit type, and duration can all
349 impact temporal PAC dissolution trends. Few studies have reported PAC concentrations
350 in water following a dilbit spill. For instance, Stoyanovich et al. (2019) tracked PACs in

the water column following spills of CLB into freshwater tanks (~1400 L and 3.1 m^2) at an oil: water ratio of 1:8000 over 11 days. Ortmann et al. (2020) report PACs in the water column following spills of three different types of dilbit (Access Western Blend, Western Canadian Select, and Synbit) during the summer into flume tank enclosures (~250 L and 0.31 m^2) filled with natural seawater for 14 days. All of the maximum water column concentrations of the seven major PAC groups (NAP, PHEN, DBT, FLU, FLA, BNT, and CHR) of both studies, as well as comparisons with our results can be found in SI Table S3. When comparing our results to previous studies at comparable oil:water ratios, the maximum concentrations for each PAC group reported for our study herein are typically greater than those of Stoyanovich et al. (2019), in all cases except for naphthalenes. Maximum naphthalene concentrations reported here were much lower than those of Ortmann et al. (2020). In general our results were in keeping with the Access Western Blend (AWB) dilbit results, but considerably lower than Synbit and Western Canadian Select (WCS) results (SI Table S3). A major difference between the present study and the tank based studies of both Stoyanovich et al. (2019) and Ortmann et al. (2020) is scale. Our lower profile, in-lake study along with the large surface area of the limnocorrals (~75 m^2) allows for wind to play a major role in the distribution of the slicks on the water's surface (Stoyanovich et al., 2021). This creates large areas of open water that promoted the volatilization of low molecular weight (LMW) compounds and is a likely explanation as to why our $\Sigma NAP_{C0\text{-}C4}$ concentrations were lower. Perhaps the most important factor to consider is chemical composition of the different dilbits. Ortmann et al. (2020) noted that the diluent differs across their three test dilbits, the composition of which can impact what PACs are found in the water

column. As shown by Ortmann et al. (2020), the type of dilbit used affects the dissolution patterns of PACs. In this case, a quantitative comparison between studies is difficult since the test dilbits were different.

3.2 Hydrocarbon Contamination of the Sediments

Sediment samples retrieved from jars placed within the limnocorrals allowed us to track temporal changes in concentration of oil components following the spills (Figure 3). The individual PAC profiles in contaminated sediments gradually increased throughout the experiment, showing no clear signs of stabilization. The accumulation of alkylated PACs in the sediments was proportional to log K_{OW} (SI Figure S9), such that PACs with higher log K_{OW}, such as those with more rings and alkyl groups, were found at higher concentrations, reflective of their affinity for the organic phase (Achten and Andersson, 2015).

Phenanthrenes were the most abundant PAC group ($\Sigma PHEN_{C0\text{-}C4}$) in the 180, 42, 18, 5.5, and 1.5 L treatments accounting for 16 – 51 % of the ΣPAC_{46}, whereas the benzonaphthothiophenes ($\Sigma BNT_{C0\text{-}C4}$) were the most abundant in the 82 and 2.9 L treatments accounting 24 – 36 % of the ΣPAC_{46} (SI Figure S10B). Notably, sediment samples collected from the dilbit treatments were enriched in sulfur heterocycles (dibenzothiophene and benzonaphthothiophenes) while the controls were not. These sulfur containing compounds are present in CLWB (SI Figure S7), which are major components of the organic sulfur content of crude oils (Mössner and Wise, 1999) and bitumen (Lam et al., 2012), and are often used as a marker for oil contamination.

The signals of naphthalenes and phenanthrenes present both in pre-spill and control samples (SI Figure S11) are likely attributable to recent and past forest fires (Murphy and Morrison, 2014), which are common during the summer months in this region. The majority of the alkylated 3-4-ring PACs remained at or below detection limits in the controls but showed elevated concentrations in the dilbit-amended treatments. Among the measurable PACs, concentrations of C_3-DBTs reached the highest concentrations in the 180, 82, and 18 L treatments (14.2, 15.4, and 19.4 ng/g d.w., respectively), C_3-BNTs reached the highest concentration in the 42 and 2.9 L treatments (10.5 and 7.9 ng/g d.w., respectively), C_2-BNTs reached the highest concentration in the 1.5 L treatment (4.3 ng/g d.w.), and C_3-NAPs reached the highest concentration in the 5.5 L treatment (4.5 ng/g d.w.) (SI Figure S11). In nearly all treatments, the maximum PAC concentrations were reached at the end of the experiment.

In sediments in direct contact with dilbit globules collected on day 70, ΣPAC_{46} concentrations were 1873 ± 2457 ng/g d.w. and 5643 ± 7817 ng/g d.w., in the 18 L and 82 L respectively (SI Figure S12). The most abundant PAC groups in both treatments were $\Sigma PHEN_{C0\text{-}C4}$, $\Sigma BNT_{C0\text{-}C4}$ and $\Sigma DBT_{C0\text{-}C3}$, whose concentrations ranged from 398 ± 536 to 512 ± 631 ng/g in the 18 L and 1385 ± 1994 to 1621 ± 2197 ng/g in the 82 L treatment (Figure 5A). The $\Sigma FLA_{C0\text{-}C4}$, $\Sigma FLU_{C0\text{-}C3}$, $\Sigma CHR_{C0\text{-}C2}$, and $\Sigma NAP_{C0\text{-}C4}$ remained at comparatively lower concentrations ranging from 87.3 ± 117 to 144 ± 174 ng/g in the 18 L and 142 ± 105 to 356 ± 497 ng/g in the 82 L treatment (SI Figure S12). The high variation among triplicate samples, evidenced by the large error bars in SI Figure S12,

418 can be explained by the uneven distribution of dilbit on the sediment surface of the
419 limnocorrals.
420 Our study uniquely captured two different aspects of sediment contamination
421 following a dilbit spill in that sediments can accumulate PACs by means of natural
422 partitioning or deposition from the water (as represented by non-oiled sediment jar
423 samples) or by direct contact with submerged oil (as represented by oiled sediment core
424 samples). These results highlight the variability in sediment PAC concentrations that
425 can arise if the dilbit submerges. For example, ΣPAC_{46} ranged from 379 – 4708 ng/g in
426 the 18 L treatment, roughly 2 – 25X higher than the maximum values observed across
427 all jar samples. In the 82 L treatment, ΣPAC_{46} concentrations ranged from 587 – 14,646
428 ng/g d.w., roughly 3 – 77X higher than maximum values observed across all jar samples
429 (SI Table S4). Evidences from the July 2007 dilbit spill in Burnaby, British Columbia,
430 Canada show maximum total PAC concentrations in oiled sediments reaching 30,300
431 ng/g d.w. (Stantec, 2012). Further, oiled sediment samples collected following the 2010
432 Kalamazoo River spill in Marshall, Michigan, U.S. show sediment total PAC
433 concentrations ranging from 7,000 to 170,000 ng/g (Fitzpatrick et al., 2012). These
434 results suggest that our study only captures a small range of potential sediment PAC
435 concentrations. Further, since dilbit sinks in a heterogeneous manner (Stoyanovich et
436 al., 2021), certain sections of the sediments will be more oiled than others, stressing the
437 need for a broad sampling approach to capture the full range of contamination.
438
439 *3.3 Chemical Source Modelling of the Water Column and Sediments*

Principal component analysis enabled us to highlight similarities and differences in the chemical profile of PACs in the water column of limnocorrals (Figure 4A). This analysis revealed that pre-spill water samples were similar across treatments, reflective of background PAC concentrations dominated by naphthalenes. Following the dilbit additions, the controls remained clustered with the pre-spill samples, while the dilbit-treatments began to shift away from pre-spill conditions. Interestingly, day 8 samples demonstrated a shift in the direction of the unweathered source CLWB. The day 8 water samples exhibited an enrichment of less soluble hydrocarbons including the 3- or greater number of ring PACs (SI Figure S6) and water-insoluble cyclic alkanes, such as hopanes, terpanes, and steranes (SI Figure S13), which is indicative of the presence of oil droplets in the sample. The water column likely experienced a flux of oil droplets forced into the water column following a rain event that occurred on day 7 (25 mm in 6 hours). Day 8 water samples also showed a biomarker profile that resembled CLWB (SI Figure S14), further suggesting the presence of droplets. Aside from day 8 samples, the other timepoints did not shift towards the source oil, likely because the water samples were dominated by water soluble compounds, whereas the source oil contained a significant proportion of high-molecular-weight (HMW) PACs that would not transfer into the water.

Similar to water samples, we used the same multivariate approach to assess the distribution of PACs in collected sediment samples. All sediment samples collected during the first week of the study clustered together along with the controls (Figure 4B). Concentrations of PACs in sediments largely remained below detection limit for the first 15 days of the study, and then began to increase, likely coinciding with dilbit

submergence (Stoyanovich et al., 2021). Between weeks 1 and 2, the PAC profiles of the samples began to change, as shown by the distancing of these points from the earlier timepoints on the PCA plot. For the remainder of the study, the PAC profiles of collected sediments shifted towards that of the CLWB source dilbit. The major forces driving hydrocarbons to the sediments are likely a combination of dispersion/diffusion from the water-accommodated phase and dilbit sedimentation.

3.4 Hydrocarbons in the Air

Our methods enabled a total of 40 parent and alkylated PAC compounds (denoted as ΣPAC_{40}) to be quantified in air (SI Table S1). Pre-spill air samples were highly variable across the three studied limnocorrals (180 L, 18 L, and NFC), with ΣPAC_{40} concentrations ranging from 1133 to 2100 ng m^{-3}. Following the spills, ΣPAC_{40} concentrations in the 180 L treatment increased from 2099 ng m^{-3} (pre-spill) to a maximum concentration of 6835 ng m^{-3} by day 2 (3.3X greater than pre-spill) and then subsequently decreased (SI Figure S15). In the 18 L treatment, ΣPAC_{40} concentrations increased from 1132 ng m^{-3} (pre-spill) to a maximum value of 3210 ng m^{-3} after just 6 hours (2.8X greater than pre-spill) and then immediately decreased, followed by a slight increase between day 2 and 8. Following the spills, the ΣPAC_{40} concentrations were comprised of between 64 – 90% and 56 – 89% naphthalene's in the 180 and 18 L treatments respectively (SI Figure S15B). These result are similar to those of Tidwell et al. (2016), who found that naphthalenes made up 90% of the total airborne PAC measurements 11 days following the *Deepwater Horizon* spill in 2010. The NFC also exhibited a slight increase from background levels of 1907 to 3030 ng m^{-3} by day 1

(1.6X greater than background; SI Figure S14A). The ΣPAC_{40} concentrations in the control however were dominated by a wider variety of compounds, with the EPA PACs, ΣFLA_{C0-C4}, $\Sigma PHEN_{C0-C4}$, and ΣDBT_{C0-C3} making up the majority of ΣPAC_{40} (SI Figure S15B).

Throughout our experiment, the only compounds that showed a clear increase in the air column over time were the naphthalenes (Figure 5) which is reflective of their volatility. The ΣNAP_{C0-C4} concentrations in the 180 L treatment increased from 730 ng m^{-3} (pre-spill) to 4916 ng m^{-3} after just 2 days, while the 18 L treatment increased from 814 ng m^{-3} (pre-spill) 2002 ng m^{-3} after just 1 day (Figure 5). The NFC also showed evidence of ΣNAP_{C0-C4} concentration increases from 569 ng m^{-3} (pre-spill) to 1278 ng m^{-3} after 4 days, suggesting that the dilbit treatments applied to limnocorrals in close proximity to this control may have influenced air column concentrations.

The temporal progression of individual parent and alkylated naphthalenes demonstrated slightly different trends across each treatment and control. In the 180 L treatment, C_2-NAP were most abundant group (1710 ng m^{-3} on day 1), followed by C_3>C_1>C_4>C_0. In the 18 L treatment, C_2-NAP were also most abundant (674 ng m^{-3} on day 1), followed by C2>C3>C4>C1>C0. Finally, in the NFC, C3-NAP was the most abundant group (354 ng m^{-3} on day 4), followed by C4>C2>C0>C1 (SI Figure S16).

Following the onset of the spills, the 180 and 18 L treatments began to exhibit a bell-shaped distribution of alkylated naphthalenes (SI Figure S16), which is indicative of a petrogenic PAC source (Murphy and Morrison, 2014). This bell-shaped pattern was not observed in the NFC. Since air sampling was carried out in an open system, it is difficult to discern any treatment specific trends. Depending on wind patterns, it is

entirely possible that surrounding treatments influenced the PAC profiles of the sampled treatments, which could explain why the NFC exhibited spikes in naphthalenes at times. Furthermore, since air sampling was only carried out from northern edge of the limnocorrals, we are not capturing the entirety of the air column above each limnocorral, which have a surface area of 75 m^2, and are likely underestimating the PAC levels in the air, especially during the early stages of evaporation. We acknowledge that the volatilization of PACs, particularly the more volatile 2-ring compounds, may have continued after the cessation of air sampling on day 8, and would require a longer sampling timeline in future studies. Regardless of the potential caveats mentioned above, these data highlight the early partitioning of the naphthalenes from the dilbit slick to the air column and may provide useful for mass transfer modelling in the future.

3.5 *Hydrocarbons in the Water Column and Sediments Predicted by Size of Spill*

Our regression design offers us the unique ability to analyze the relationship between oil components in environmental samples and the individual oil:water ratios using simple linear regressions. A positive slope would indicate that as the ratio of dilbit to water increases, the concentrations of PACs in the water column will increase. We observed a significant positive relationship emerge at the majority of timepoints > 8 days for $\Sigma PAC_{46,}$ $\Sigma NAP_{C0\text{-}C4}$, $\Sigma FLU_{C0\text{-}C3}$, $\Sigma FLA_{C0\text{-}C4}$, $\Sigma BNT_{C0\text{-}C4}$, and $\Sigma CHR_{C0\text{-}C3}$ (Figure 6, SI Figure S17). The PAC groups $\Sigma PHEN_{C0\text{-}C4}$ and $\Sigma DBT_{C0\text{-}C3}$ did not yield significant positive relationships until the end of the experiment (Figure 6C-D). SI Figure S17 further highlights the dynamics of concentration change across spill volumes, specifically the linearity of the relationship between PAC concentrations and oil:water

ratios. This figure also shows how the 18 L treatment, which had the highest leakage rate of all the limnocorrals (0.035 d^{-1}; Rodriques et al. 2021), is recurrently found below the regression line for each compound group and sampling timepoint. This suggests that the water exchange occurring between the limnocorral and the lake was likely diluting the observed PAC concentrations.

Unlike water column PAC concentrations, accumulation trends of PACs in the sediments over the 70 days were found to be similar among treatments at most timepoints (Figure 3). While the majority of the regression slopes were positive, significant relationships were only observed between $\Sigma NAP_{C0\text{-}C4}$ and oil:water ratio on days 42 and 70 (Figure 7, SI Figure S18). We conclude that the amount of dilbit spilled has less effect on the concentration of naturally dispersed PACs in the sediments compared to the water column within the 70 day study timeline. Other factors aside from spill volume may be limiting accumulation in the sediment. As previously noted, accumulation in the sediments was proportional to the $\log K_{OW}$ value of PACs. Since these compounds do not readily dissolve in water, they would have to reach the sediments by other means, including through the dispersion of oil droplets. Therefore, the accumulation of these HMW compounds in the sediments is likely limited by the compounds migrating through the water column via droplets, which is unrelated to spill volume. By incorporating the oil:water ratio of each individual spill as the independent variable in the regressions, the generated linear models (SI Table S5 and S6) can be used to predict PAC contamination at different volumetric scales of dilbit spills that occur in boreal lakes under similar environmental conditions and timelines as the present study.

555

556 *3.6 PAC Mass Balance*

557 We utilized a field mass balance to determine how the water column and
558 sediment results compare to what would be expected based on total dissolvable
559 compound masses in the spilled oil using a similar approach to Brussaard et al. (2016).
560 Since the air samples do not reflect the concentrations of PACs in the entire air column
561 above the 75 m^2 limnocorrals, we omitted these data from the mass balance. The
562 change in water volume of each limnocorral has previously been reported by Rodriguez-
563 Gil et al. (2021) and we estimated sediment volume using the dimensions of the
564 limnocorral base (approx. 75 m^2) and the nominal sediment sampling depth (0.05 m).
565 We used the timepoint of highest measured concentrations for the 7 alkylated PAC
566 groups and ΣPAC_{46} in the water column and sediments to determine which percentage
567 of the spilled chemical components are accounted for in the environmental samples
568 (Table 1). The water column showed between 0.02 – 1 % of ΣPAC_{46}, 0.02 – 0.6 % of
569 $\Sigma NAP_{C0\text{-}C4}$, 0.01 – 1.3 % of $\Sigma PHE_{C0\text{-}C4,}$ 0.01 – 2 % of $\Sigma DBT_{C0\text{-}C3}$, 0.05 – 2.1 % of $\Sigma FLU_{C0\text{-}}$
570 $_{C3}$, 0.01 – 0.7 of $\Sigma FLA_{C0\text{-}C4}$, 0.004 – 0.5 % of $\Sigma BNT_{C0\text{-}C4}$, and 0.01 – 0.3 % of $\Sigma CHR_{C0\text{-}C3}$,
571 were released from the slick into the water, across each treatment. These estimates are
572 reasonable, considering that dissolution typically only results in a fraction of a percent of
573 the oil actually dissolving into the water column (Fingas, 2015; Gros et al., 2014). The
574 sediments show between 0.1 – 5.4 % of ΣPAC_{46}, 0.1 – 4.5 % of $\Sigma NAP_{C0\text{-}C4}$, 0.2 – 8.0 %
575 of $\Sigma PHE_{C0\text{-}C4,}$ 0.1 – 3.7 % of $\Sigma DBT_{C0\text{-}C3}$, 0.1 – 7.7 % of $\Sigma FLU_{C0\text{-}C3}$, 0.1 – 6.5 of $\Sigma FLA_{C0\text{-}C4}$,
576 0.1 – 6.4 % of $\Sigma BNT_{C0\text{-}C4}$, and 0.1 – 8.6 % of $\Sigma CHR_{C0\text{-}C3}$ were detected, across each

577 treatment. Ultimately, these results demonstrate that sediments are a more prominent
578 sink for these PAC groups compared to the water column.
579
580 *3.7 Implications for Ecological Exposure Following Dilbit Spills*
581 The Canadian Council of Ministers of the Environment (CCME) provides water
582 (Canadian Council of Ministers of the Environment (CCME), 1999a) and sediment
583 (Canadian Council of Ministers of the Environment (CCME), 1999b) quality guidelines
584 for the protection of aquatic life for a variety of parent PACs, but none of the PAC
585 concentrations we observed in oil-treated limnocorrals exceed these guidelines for
586 water (SI Table S7) or sediment (SI Table S8). However, these values are not typically
587 applicable to crude oil pollution including dilbit, since dilbit is dominated by alkylated
588 PACs (Yang et al., 2018). Alkylated PACs can possess similar toxicities to that of their
589 parent compounds (Andersson and Achten, 2015; Vendrame et al., 1999) and in other
590 cases can be more toxic than their parent counterparts (Marvanová et al., 2008;
591 Turcotte et al., 2011). Therefore, while both water column and sediment samples do not
592 surpass any CCME guidelines for parent compounds (SI Table S7), we cannot
593 completely rule out the potential for toxicity of the alkylated congeners.
594 The highest ΣPAC_{46} concentration observed in the water column in our study was
595 2398 ng/L on day 70 in the 180 L treatment, which is below all reported concentrations
596 for dilbit toxicity in the literature. The toxicity of dilbit has been assessed by exposing
597 aquatic organisms to water that has been forcibly mixed with dilbit, referred to as a
598 water accommodated fraction (WAF). WAFs are thus a complex mixture of parent and
599 alkylated PACs and monoaromatics. Philibert et al. (2016) found dilbit WAFs with total

PAC concentrations above 28000 ng/L, made up of approximately 7500 ng/L ΣNAP_{C0-C4}, 1700 ng/L $\Sigma PHEN_{C0-C4}$, 1140 ng/L ΣFLU_{C0-C3}, and 2300 ng/L ΣDBT_{C0-C3} (calculated from 60% of initial WAF, individual concentrations estimated from graphs) significantly reduced survival of zebrafish embryos. Madison et al. (2017) determined 17 day median effective concentrations (EC_{50}) values for embryotoxicity of Japanese medaka to occur at ΣPAC concentrations > 3000 ng/L. Alderman et al. (2017) exposed juvenile sockeye salmon to CLB WAFs and observed the induction of biomarkers for PAC exposure at ΣPAC of 3500 ng/L but only observed impacts on swimming performance at ΣPAC concentrations > 66700 ng/L. Barron et al. (2018) exposed a variety of standard aquatic test species to CLB WAFs and obtained lowest 48 h lethal concentrations (LC_{50}) ranging from 7600 ng ΣPAC /L for Mysid (*Americamysis bahia*) to > 27000 ng ΣPAC /L for Cladocera (*Ceriodaphnia dubia*). Further, the researchers found no observable effect concentrations (NOEC) of 3670 and 5990 ng ΣPAC /L for Mysid and Cladocera, respectively, following 7 d exposures.

One aspect not considered in our study is the production of oxygenated compounds after weathering processes including biodegradation and photooxidation (Charrié-Duhaut et al., 2000; Lee et al., 2015). Weathered oil samples have demonstrated increases in oxygen containing compounds such as carboxylic acids, ketones, and esters (Aeppli et al., 2012), which can be toxic (Jones et al., 2011). Given the prolonged periods of weathering the dilbit slicks endured, it is possible that oxygenated by-products were produced.

While ΣPAC_{46} concentrations in our sediment jar samples are well below these thresholds for toxicity, the oiled sediment samples: OS-18-1, OS-18-2, and OS-82-2 (SI

623 Figure S12), all exceed this range. Barron et al. (2020) reported lowest observable
624 effect levels (LOECs) and EC50s for benthic amphipods *Hyalella azteca* and
625 *Leptocheirus plumulosus* exposed to CLB oiled sediment during 10 d survival tests. The
626 LOEC and EC50 values were 17300 and 40800 ng ΣPAC g^{-1} d.w., respectively for *H.*
627 *azteca*, and 1300 and 1400 ng ΣPAC g^{-1} d.w., respectively for *L. plumulosus* (estimated
628 from wet weight based on reported mean moisture content of 39.4%). This stresses the
629 importance of recovering spilled dilbit before submergence occurs. Our results suggest
630 that sediments that are not physically oiled do not pose a threat to aquatic biota based
631 on the current state of sediment toxicity literature. However, sediments that are in direct
632 contact with submerged dilbit can be highly contaminated with PACs, above thresholds
633 of harm to benthic organisms.
634
635 **Conclusion**
636 In conclusion, our study demonstrates that under low-energy spill scenarios
637 typical of small boreal lakes, water column PAC concentrations likely remain below
638 levels that would be toxic to aquatic biota, at least within the first 70 days after a spill
639 occurs. These findings are also mirrored in the majority of sediment samples, however,
640 elevated PAC concentrations of toxicological concern can occur in sediment is in direct
641 contact with sunken dilbit tarballs. This creates the potential of substantial long-term risk
642 to freshwater benthic organisms, especially as evidence supporting the hypothesis that
643 dilbit can sink in freshwater continues to emerge. In addition, PAC concentrations are
644 enriched in alkylated PAC homologs for which toxicity thresholds are not fully
645 developed. Future work should determine toxicity thresholds for alkylated PACs as we

have shown these compounds dominate chemical profile of water and sediment samples following dilbit spills into the freshwater environment.

Acknowledgements

This is contribution No. 7 of the BOREAL study. Funding for the study was provided by a Natural Sciences and Engineering Research Council Strategic Partnership Grant (STPGP 493786-16 awarded to J.M. Blais, M. Hanson, and D.M. Orihel), a grant under the Oceans Protection Program, in-kind contributions from Environment and Climate Change Canada (ECCC), and in-kind support from the IISD-Experimental Lakes Area. A special thank you to J. Séguin, T. Black, J. Cederwall, L. Timlick, S. Patterson, J. Mason, D. Denton, H. Kosichek, K. Watson, and D. Dey for their contributions to the project.

Table & Figure Captions

Table 1. Environmental mass balance of PAC groups in the water column and sediments. Percentages are reflective of the maximum concentration observed in the water column and sediments for each PAC group.

Media	Compound Class	Percent Detected (%)						
		180 L	82 L	42 L	18 L	5.5 L	2.9 L	1.5 L
Water[a]	ΣPAC_{46}	0.02	0.03	0.1	0.1	0.3	0.3	1.1
	$\Sigma NAP_{C0\text{-}C4}$	0.02	0.04	0.1	0.1	0.4	0.3	0.6
	$\Sigma PHE_{C0\text{-}C4}$	0.01	0.02	0.1	0.1	0.3	0.5	1.3
	$\Sigma DBT_{C0\text{-}C3}$	0.01	0.02	0.1	0.1	0.3	0.4	2.0
	$\Sigma FLU_{C0\text{-}C3}$	0.05	0.1	0.2	0.2	0.6	0.6	2.1
	$\Sigma FLA_{C0\text{-}C4}$	0.01	0.02	0.03	0.1	0.2	0.2	0.7
	$\Sigma BNT_{C0\text{-}C4}$	0.004	0.01	0.02	0.03	0.1	0.1	0.5
	$\Sigma CHR_{C0\text{-}C3}$	0.01	0.02	0.02	0.05	0.1	0.2	0.3
Sediment[b]	ΣPAC_{46}	0.1	0.2	0.4	1.4	1.2	3.7	5.4
	$\Sigma NAP_{C0\text{-}C4}$	0.1	0.1	0.2	0.5	1.2	2.1	4.5
	$\Sigma PHE_{C0\text{-}C4}$	0.2	0.3	0.5	2.0	1.9	5.5	8.0
	$\Sigma DBT_{C0\text{-}C3}$	0.1	0.2	0.3	1.3	0.8	3.0	3.7
	$\Sigma FLU_{C0\text{-}C3}$	0.1	0.2	0.4	1.1	1.1	3.6	7.7
	$\Sigma FLA_{C0\text{-}C4}$	0.1	0.3	0.5	1.7	1.2	3.0	6.5
	$\Sigma BNT_{C0\text{-}C4}$	0.1	0.4	0.6	2.6	0.5	8.6	6.4
	$\Sigma CHR_{C0\text{-}C3}$	0.1	0.4	0.6	2.4	0.7	5.9	8.6

[a]Total water volume calculated based on modelled predictions from dynamic tritium model by Rodriguez-Gil et al. (2021)

[b]Sediment mass measurements based on assumed dry density of 2.5 g cm^{-3} (Anderson et al., 1987; Beaty, 1994; Bird et al., 1993; Crusius and Anderson, 1991; Durham and Joshi, 1984), surface area of 75 m^2, and sample depth of 0.05m.

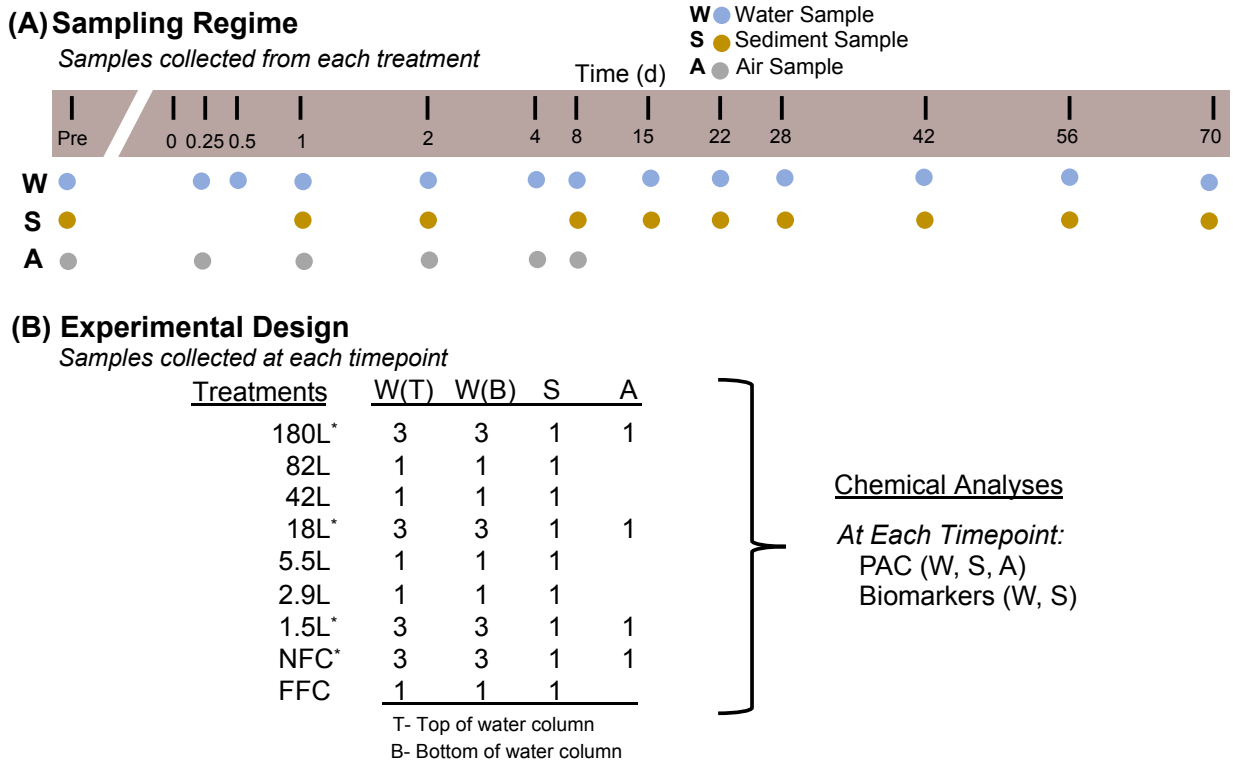

677

678 **Figure 1.** Overview of environmental media sampling timepoints and associated
679 analyses. Panel (A) shows the sampling regime for the water column (W), sediments
680 (S), and Air. Panel (B) shows the number of samples collected at each timepoint for
681 each environmental medium (34 water samples, 9 sediment samples, and 4 air
682 samples- at each timepoint). TPH: total petroleum hydrocarbons, TSH: total saturated
683 hydrocarbons, TAH: total aromatic hydrocarbons.

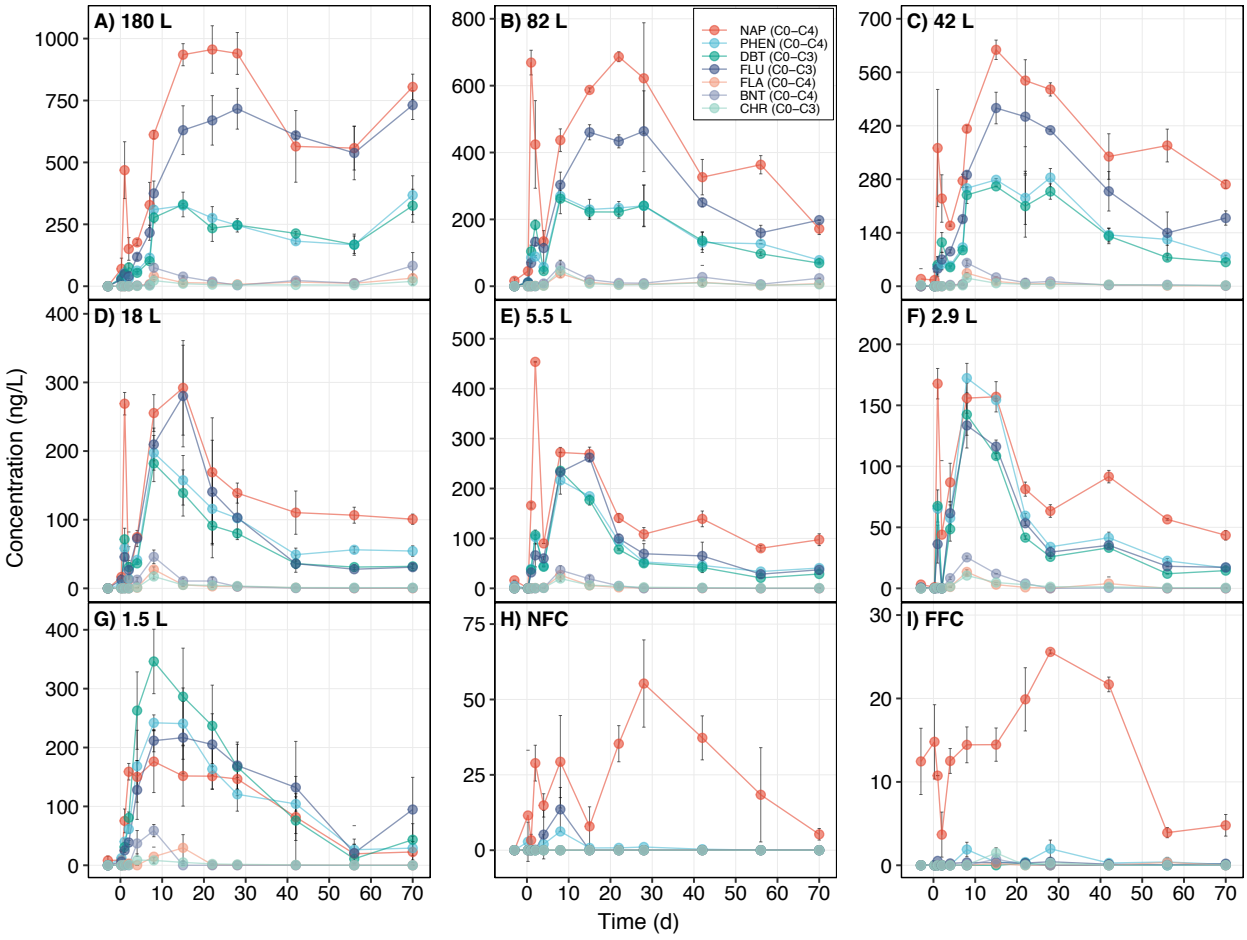

684

685 **Figure 2.** Polycyclic aromatic compound (PAC) group concentrations in the water
686 column over time. The sum of the parent and each alkylated homolog in each group is
687 presented. Error bars represent standard deviation measured over n= 6 (180 L, 18 L,
688 1.5 L, and NFC) and n = 2 (82 L, 42 L, 5.5 L, 2.9 L, and FFC). Note changing y-axis
689 scale.

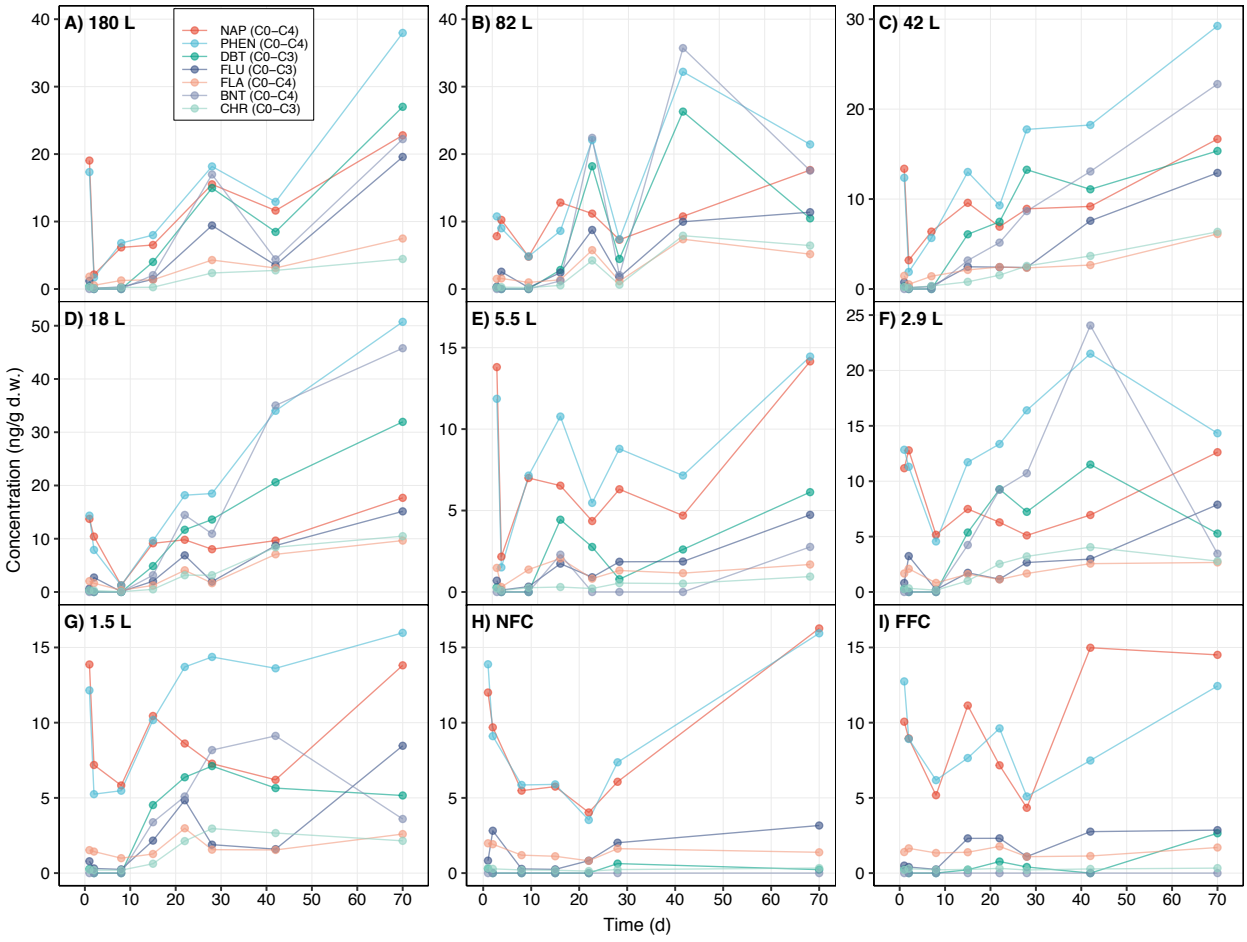

690

691 **Figure 3.** Polycyclic aromatic compound (PAC) group concentrations over time in the

692 sediments. The sum of the parent and each alkylated homolog in each group is

693 presented. Note changing y-axis scale.

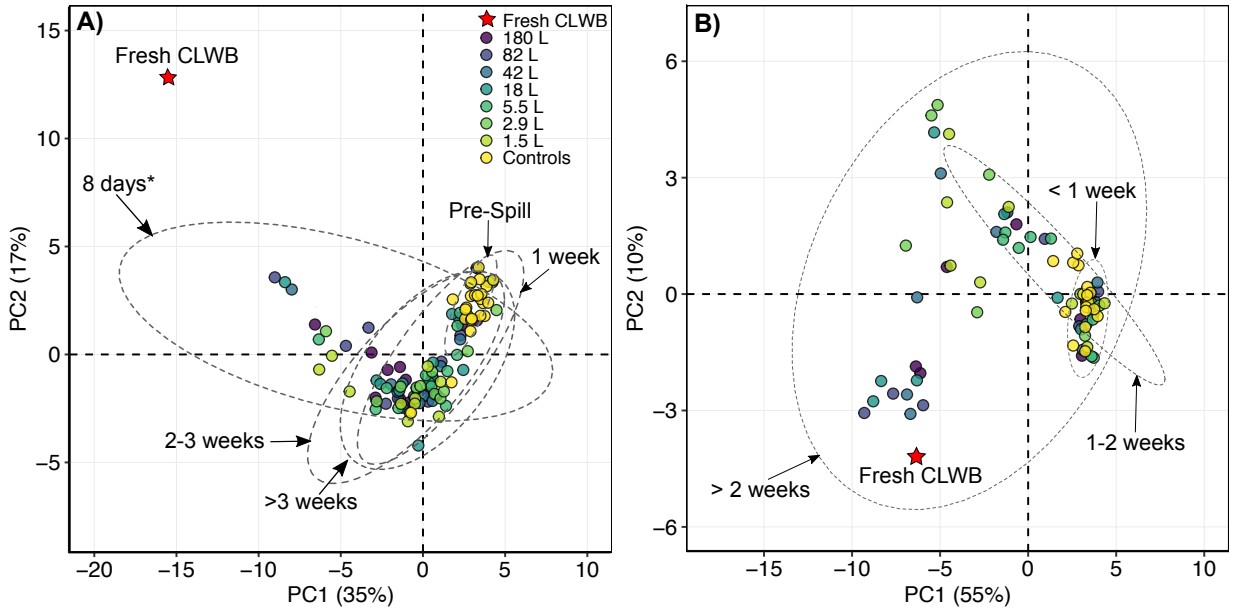

694

695 **Figure 4.** Principal component analysis of the PAC profiles normalized to ΣPAC_{46} in
696 water (A) and sediment (B) samples collected throughout the entire study from each
697 treatment and control. Principal components 1 and 2 account for 52% of the variability in
698 the data set in panel A and 65% of the variability in the data set in panel B. Ellipses
699 represent the 95% confidence interval within the 2-D space.

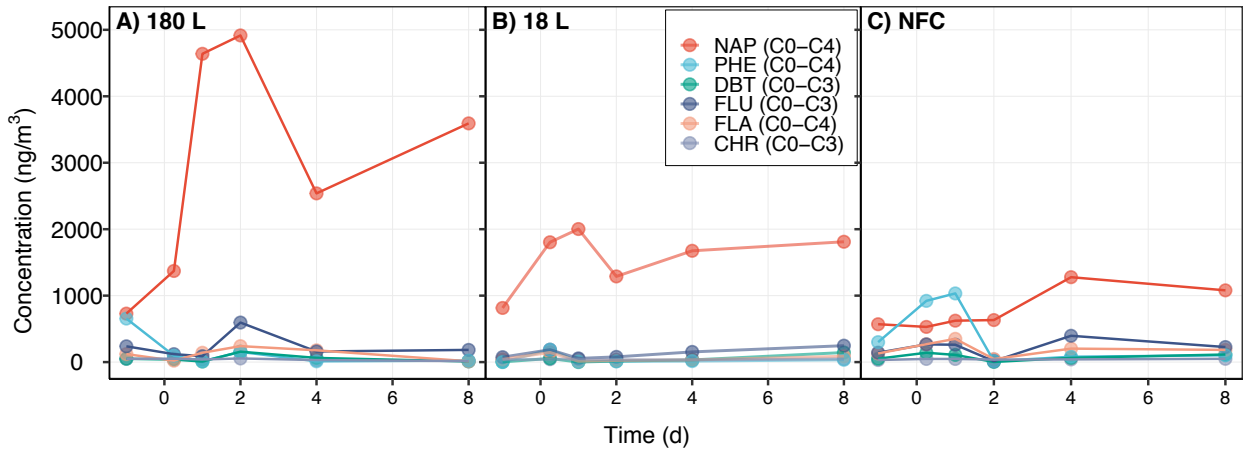

700

701 **Figure 5.** PAC for homolog family concentrations over time in the air column above the
702 180 L (A), 18 L (B), and NFC (C) treatments. The sum of the parent and each alkylated
703 homolog group is presented.

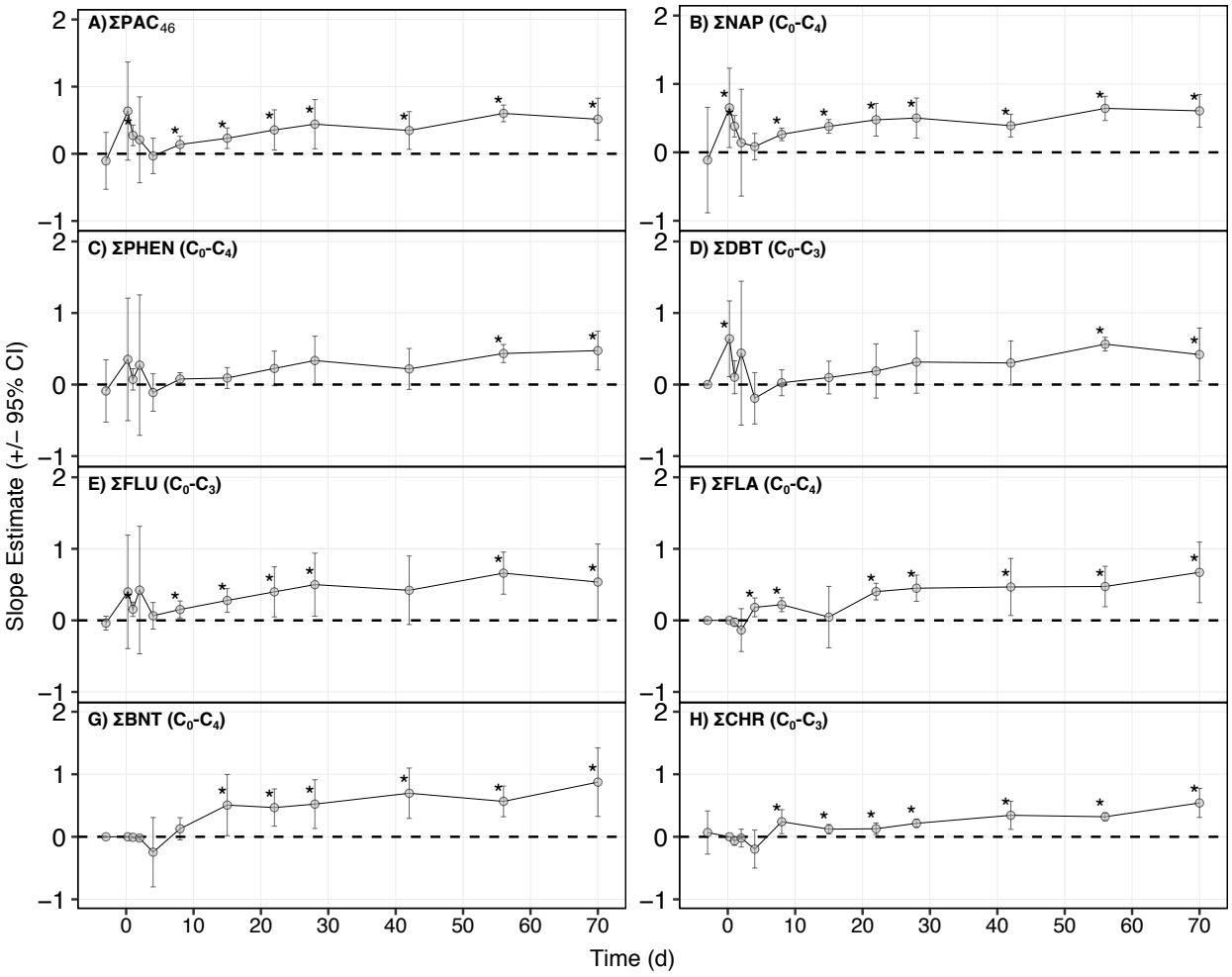

Figure 6. Regression slope estimates obtained by linear regression of log transformed oil:water ratio for of each treatment against the log transformed concentration in the water column of each PAC group. Regression parameters are presented in Table S5. Asterix' represent slopes that are significantly different than 0 at an alpha level of 0.05.

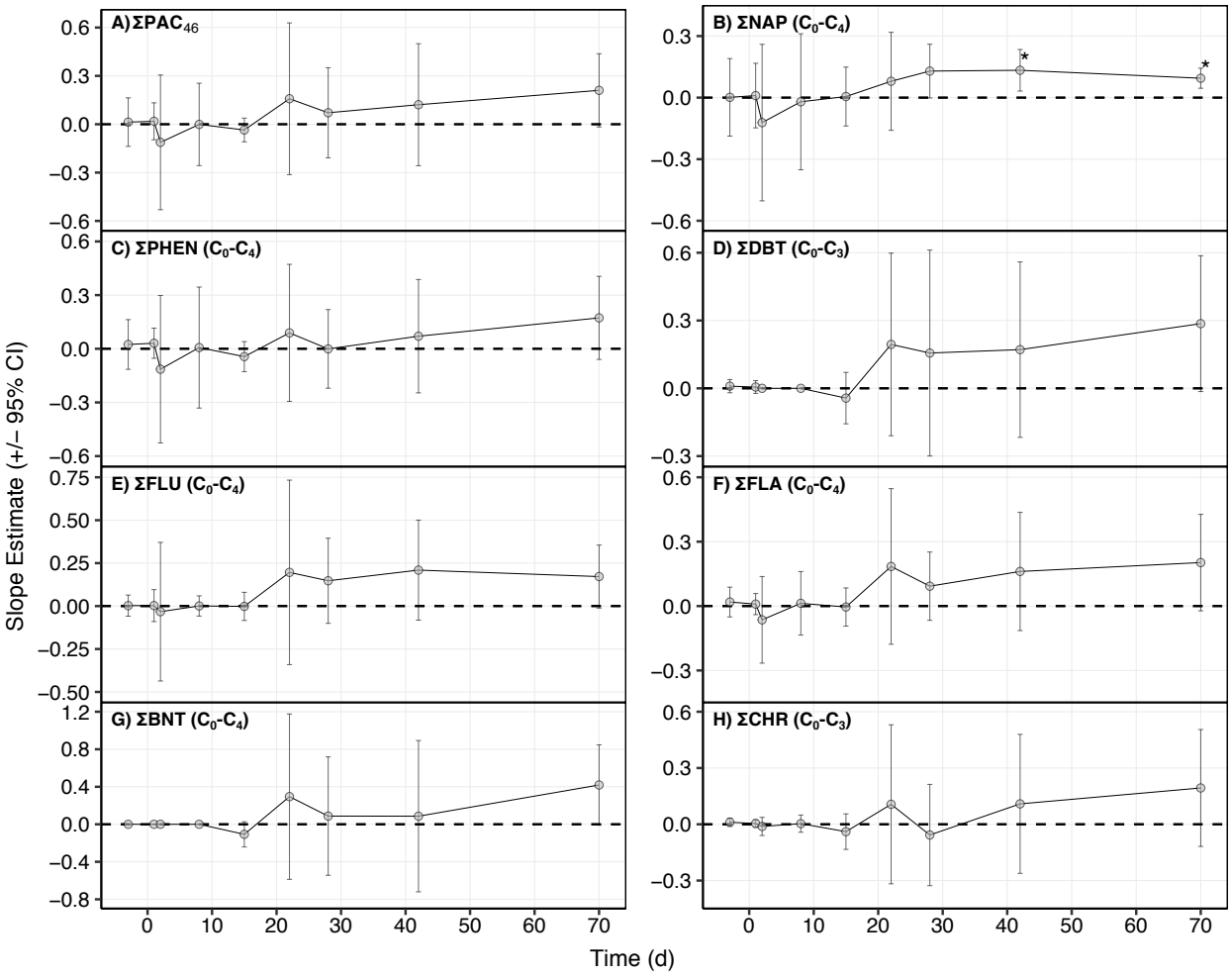

Figure 7. Regression slopes obtained by linear regression of log transformed oil:water ratio of each treatment against the log transformed concentration in the sediments of each polycyclic aromatic compound (PAC) group. Regression parameters are presented in Table S6. Asterix' represent slopes that are significantly different than 0 at an alpha level of 0.05.

References

Achten, C., Andersson, J.T., 2015. Overview of Polycyclic Aromatic Compounds (PAC). Polycycl. Aromat. Compd. 35, 177–186. https://doi.org/10.1080/10406638.2014.994071

Aeppli, C., Carmichael, C.A., Nelson, R.K., Lemkau, K.L., Graham, W.M., Redmond, M.C., Valentine, D.L., Reddy, C.M., 2012. Oil weathering after the Deepwater Horizon disaster led to the formation of oxygenated residues. Environ. Sci. Technol. 46, 8799–8807.

Alderman, S.L., Lin, F., Farrell, A.P., Kennedy, C.J., Gillis, T.E., 2017. Effects of diluted bitumen exposure on juvenile sockeye salmon: from cells to performance. Environ. Toxicol. Chem. 36, 354–360.

Allan, S.E., Smith, B.W., Anderson, K.A., 2012. Impact of the Deepwater Horizon oil spill on bioavailable polycyclic aromatic hydrocarbons in Gulf of Mexico coastal waters. Environ. Sci. Technol. 46, 2033–2039.

Andersson, J.T., Achten, C., 2015. Time to say goodbye to the 16 EPA PAHs? Toward an up-to-date use of PACs for environmental purposes. Polycycl. Aromat. Compd. 35, 330–354. https://doi.org/10.1080/10406638.2014.991042

Baca, B.J., Getter, C.D., 1985. Freshwater oil spill considerations: protection and cleanup, in: International Oil Spill Conference. American Petroleum Institute, pp. 385–390. https://doi.org/10.7901/2169-3358-1985-1-385

Barron, M.G., Conmy, R.N., Holder, E.L., Meyer, P., Wilson, G.J., Principe, V.E., Willming, M.M., 2018. Toxicity of Cold Lake Blend and Western Canadian Select dilbits to standard aquatic test species. Chemosphere 191, 1–6.

Barron, M.G., Moso, E.M., Conmy, R.N., Meyer, P., Sundaravadivelu, D., 2020. Toxicity of sediment oiled with diluted bitumens to freshwater and estuarine amphipods. Mar. Pollut. Bull. 163, 111941.

Bejarano, A.C., Clark, J.R., Coelho, G.M., 2014. Issues and challenges with oil toxicity data and implications for their use in decision making: A quantitative review. Environ. Toxicol. Chem. 33, 732–742.

Brussaard, C.P., Peperzak, L., Beggah, S., Wick, L.Y., Wuerz, B., Weber, J., Arey, J.S., Van Der Burg, B., Jonas, A., Huisman, J., 2016. Immediate ecotoxicological effects of short-lived oil spills on marine biota. Nat. Commun. 7, 1–11.

Canadian Council of Ministers of the Environment (CCME), 1999a. Canadian water quality guidelines for the protection of aquatic life: Polycyclic aromatic hydrocarbons (PAHs), In: Canadian environmental quality guidelines. Canadian Council of Ministers of the Environment, Winnipeg.

Canadian Council of Ministers of the Environment (CCME), 1999b. Canadian sediment quality guidelines for the protection of aquatic life: Polycyclic aromatic hydrocarbons (PAHs), In: Canadian environmental quality guidelines. Canadian Council of Ministers of theEnvironment, Winnipeg.

CAPP, 2019. 2019 Crude Oil Forecast, Markets and Transportation (No. 2019– 0018). Canadian Association of Petroleum Producers (CAPP), Calgary, AB.

Charrié-Duhaut, A., Lemoine, S., Adam, P., Connan, J., Albrecht, P., 2000. Abiotic oxidation of petroleum bitumens under natural conditions. Org. Geochem. 31, 977–1003.

760 Crosby, S., Fay, R., Groark, C., Smith, J.R., Sullivan, T., Pavia, R., Shigenaka, G., 2013.
761 Transporting Alberta oil sands products: defining the issues and assessing the risks (No.
762 NOAA Technical Memorandum NOS OR&R 43). U.S. Dept. of Commerce, Seattle, WA:
763 Emergency Response Division, NOAA.
764 Debruyn, A.M., Wernick, B.G., Stefura, C., McDonald, B.G., Rudolph, B.-L., Patterson, L.,
765 Chapman, P.M., 2007. In situ experimental assessment of lake whitefish development
766 following a freshwater oil spill. Environ. Sci. Technol. 41, 6983–6989.
767 https://doi.org/10.1021/es0709425
768 Fingas, M., 2015. Review of The Properties and Behaviour of Diluted Bitumen, in: Proceeding of
769 the 39th Arctic and Marine Oil-Spill Program Technical Seminar. Environment and
770 Climate Change Canada, Vancouver, B.C., Canada, pp. 470–494.
771 Fingas, M., Fieldhouse, B., 2009. Studies on crude oil and petroleum product emulsions: Water
772 resolution and rheology. Colloids Surf. Physicochem. Eng. Asp. 333, 67–81.
773 Fitzpatrick, F., Bejarano, A., Michel, J., Williams, L., 2012. Net Environmental Benefit Analysis
774 (NEBA) Relative Risk Ranking Conceptual Design: Kalamazoo River System, Enbridge Line
775 6B MP 608 Marshall, MI Pipeline Release. U.S. Geological Survey, Reston, Virginia.
776 Fitzpatrick, F.A., Boufadel, M.C., Johnson, R., Lee, K.W., Graan, T.P., Bejarano, A.C., Zhu, Z.,
777 Waterman, D., Capone, D.M., Hayter, E., 2015. Oil-particle interactions and
778 submergence from crude oil spills in marine and freshwater environments: Review of
779 the science and future research needs (No. 2015–1076). US Geological Survey.
780 Gros, J., Nabi, D., Würz, B., Wick, L.Y., Brussaard, C.P., Huisman, J., van der Meer, J.R., Reddy,
781 C.M., Arey, J.S., 2014. First day of an oil spill on the open sea: Early mass transfers of
782 hydrocarbons to air and water. Environ. Sci. Technol. 48, 9400–9411.
783 https://doi.org/10.1021/es502437e
784 Husky Energy Inc, 2016. North Saskatchewan River Water Source Risk Assessment Report.
785 Jones, D., Scarlett, A.G., West, C.E., Rowland, S.J., 2011. Toxicity of individual naphthenic acids
786 to Vibrio fischeri. Environ. Sci. Technol. 45, 9776–9782.
787 Kennon, M.E., Bouldin, J.L., 2015. Aquatic Effects of a Localized Oil Spill on Lake Conway, AR and
788 Its Tributaries. J. Ark. Acad. Sci. 69, 60–67.
789 King, T.L., Robinson, B., Boufadel, M., Lee, K., 2014. Flume tank studies to elucidate the fate and
790 behavior of diluted bitumen spilled at sea. Mar. Pollut. Bull. 83, 32–37.
791 https://doi.org/10.1016/j.marpolbul.2014.04.042
792 King, T.L., Robinson, B., Lee, K., Li, H., Boufadel, M.C., Clyburne, J.A., 2019. Seasonal Effect Data
793 on Monocyclic Aromatics Dissolution from Surface Spills of Bitumen Blends: Implications
794 for Environmental Risk Assessments, in: Proceedings of the Forty-Second AMOP
795 Technical Seminar. Environment and Climate Change Canada, Ottawa, ON, Canada, pp.
796 773–790.
797 Lam, V., Li, G., Song, C., Chen, J., Fairbridge, C., Hui, R., Zhang, J., 2012. A review of
798 electrochemical desulfurization technologies for fossil fuels. Fuel Process. Technol. 98,
799 30–38.
800 Lee, K. (chair), Boufadel, M., Chen, B., Foght, J., Hodson, P., Swanson, S., Venosa, A., 2015.
801 Expert Panel Report on the Behaviour and Environmental Impacts of Crude Oil Released
802 into Aqueous Environments (No. ISBN: 978-1-928140-02-3). Royal Society of Canada,
803 Ottawa, ON, Canada.

Lee, K., Prince, R.C., Greer, C.W., Doe, K.G., Wilson, J.E.H., Cobanli, S.E., Wohlgeschaffen, G.D., Alroumi, D., King, T., Tremblay, G.H., 2003. Composition and toxicity of residual Bunker C fuel oil in intertidal sediments after 30 years. Spill Sci. Technol. Bull. 8, 187–199.

Madison, B.N., Hodson, P.V., Langlois, V.S., 2017. Cold Lake Blend diluted bitumen toxicity to the early development of Japanese medaka. Environ. Pollut. 225, 579–586.

Marvanová, S., Vondrácek, J., Pěnččíková, K., Trilecová, L., Krčmářř, P., Topinka, J., Nováková, Z., Milcová, A., Machala, M., 2008. Toxic effects of methylated benz [a] anthracenes in liver cells. Chem. Res. Toxicol. 21, 503–512.

Mössner, S.G., Wise, S.A., 1999. Determination of polycyclic aromatic sulfur heterocycles in fossil fuel-related samples. Anal. Chem. 71, 58–69.

Murphy, B.L., Morrison, R.D., 2014. Introduction to environmental forensics. Academic Press.

NASEM, 2016. Spills of Diluted Bitumen from Pipelines: A Comparative Study of Environmental Fate, Effects, and Response (No. ISBN: 978-0-309-38010-2). National Academies of Sciences, Engineering and Medicine (NASEM), Washington, DC.

NEB, 2017. Incident Data. National Energy Board. Government of Canada, Calgary, AB.

Neff, J.M., Stubblefield, W.A., 1995. Chemical and toxicological evaluation of water quality following the Exxon Valdez oil spill, in: Exxon Valdez Oil Spill: Fate and Effects in Alaskan Waters. ASTM International.

Ortmann, A.C., Cobanli, S.E., Wohlgeschaffen, G., MacDonald, J., Gladwell, A., Davis, A., Robinson, B., Mason, J., King, T.L., 2020. Measuring the fate of different diluted bitumen products in coastal surface waters. Mar. Pollut. Bull. 153, 111003.

Owens, E.H., Taylor, E., Marty, R., Little, D.I., 1993. An inland oil spill response manual to minimize adverse environmental impacts, in: International Oil Spill Conference. American Petroleum Institute, pp. 105–109.

Philibert, D.A., Philibert, C.P., Lewis, C., Tierney, K.B., 2016. Comparison of diluted bitumen (dilbit) and conventional crude oil toxicity to developing zebrafish. Environ. Sci. Technol. 50, 6091–6098.

Reddy, C.M., Quinn, J.G., 2001. The North Cape oil spill: hydrocarbons in Rhode Island coastal waters and Point Judith pond. Mar. Environ. Res. 52, 445–461.

Rodriguez-Gil, J.L., Stoyanovich, S., Hanson, M.L., Hollebone, B., Orihel, D.M., Palace, V., Faragher, R., Mirnaghi, F.S., Shah, K., Yang, Z., 2021. Simulating diluted bitumen spills in boreal lake limnocorrals-Part 1: Experimental design and responses of hydrocarbons, metals, and water quality parameters. Sci. Total Environ. 148537.

Saunders, L., Rodriguez-Gil, J.L., Stoyanovich, S., kimpe, L., Hanson, M., Hollebone, B., Orihel, D., Blais, J., In Prep. Effect of spilled diluted bitumen on chemical air-water exchange in boreal lake limnocorrals.

Shah, K., Watson, K., Hollebone, B., Yang, Z., Lambert, P., Faragher, R., Aljawahari, M., Dey, D., Mirnaghi, F., Stoyanovich, S., Blais, J.M., 2019. The BOREAL Project: The Design and Execution of a Controlled Oil Spill Study in a Canadian Freshwater Lake, in: Proceedings of the Forty-Second AMOP Technical Seminar. Environment and Climate Change Canada, Ottawa, ON, Canada, pp. 276–294.

Stantec, 2012. Summary of Clean up and Effects of the 2007 Spill of Oil from Trans Mountain Pipeline to Burrard Inlet (No. Project No. 1231-10505).

Stoyanovich, S., Rodríguez-Gil, J.R., Hanson, M., Hollebone, B.P., Orihel, D.M., Palace, V., Faragher, R., Mirnaghi, F.S., Shah, K., Yang, Z., 2021. Simulating diluted bitumen spills in boreal lake limnocorrals-Part 2: Factors affecting the physical characteristics and submergence of diluted bitumen. Sci. Total Environ. 148580.

Stoyanovich, S., Yang, Z., Hanson, M., Hollebone, B., Orihel, D., Palace, V., Rodriguez-Gil, J., Faragher, R., Mirnaghi, F., Shah, K., Blais, J., 2019. Simulating a spill of diluted bitumen: Environmental weathering and submergence in a model freshwater system. ET&C. https://doi.org/10.1002/etc.4600

Tarr, M.A., Zito, P., Overton, E.B., Olson, G.M., Adhikari, P.L., Reddy, C.M., 2016. Weathering of oil spilled in the marine environment. Oceanography 29, 126–135. https://doi.org/10.5670/oceanog.2016.77

Tidwell, L.G., Allan, S.E., O'Connell, S.G., Hobbie, K.A., Smith, B.W., Anderson, K.A., 2016. PAH and OPAH flux during the deepwater horizon incident. Environ. Sci. Technol. 50, 7489–7497.

Turcotte, D., Akhtar, P., Bowerman, M., Kiparissis, Y., Brown, R.S., Hodson, P.V., 2011. Measuring the toxicity of alkyl-phenanthrenes to early life stages of medaka (Oryzias latipes) using partition-controlled delivery. Environ. Toxicol. Chem. 30, 487–495.

US EPA, 2013. Dredging Begins on Kalamazoo River, Enbridge Oil Spill, Marshall, Michigan. U.S. Environmental Protection Agency (US EPA).

USDOT, 2017. Hazardous Liquid Accident Data, 2010 - 2017, In: Pipeline and Hazardous Materials Safety Administration, ed. Pipeline Data and Statistics. Washington, DC: U.S. Department of Transportation,.

Van Hamme, J.D., Singh, A., Ward, O.P., 2003. Recent advances in petroleum microbiology. Microbiol. Mol. Biol. Rev. 67, 503–549.

Vendrame, R., Braga, R.S., Takahata, Y., Galvao, D.S., 1999. Structure- activity relationship studies of carcinogenic activity of polycyclic aromatic hydrocarbons using calculated molecular descriptors with principal component analysis and neural network methods. J. Chem. Inf. Comput. Sci. 39, 1094–1104.

Venosa, A.D., Suidan, M.T., King, D., Wrenn, B.A., 1997. Use of hopane as a conservative biomarker for monitoring the bioremediation effectiveness of crude oil contaminating a sandy beach. J. Ind. Microbiol. Biotechnol. 18, 131–139. https://doi.org/10.1038/sj.jim.2900304

Yang, C., Lambert, P., Zhang, G., Yang, Z., Landriault, M., Hollebone, B., Fieldhouse, B., Mirnaghi, F., Brown, C.E., 2017. Characterization of chemical fingerprints of unconventional Bakken crude oil. Environ. Pollut. 230, 609–620. https://doi.org/0.1016/j.envpol.2017.07.011

Yang, Z., Hua, Y., Mirnaghi, F., Hollebone, B.P., Jackman, P., Brown, C.E., Yang, C., Shah, K., Landriault, M., Chan, B., 2018. Effect of evaporative weathering and oil-sediment interaction on the fate and behavior of diluted bitumen in marine environments. Part 2. The water accommodated and particle-laden hydrocarbon species and toxicity of the aqueous phase. Chemosphere 191, 145–155. https://doi.org/10.1016/j.chemosphere.2017.10.033

Yang, Z., Shah, K., Laforest, S., Hollebone, B.P., Situ, J., Crevier, C., Lambert, P., Brown, C.E., Yang, C., 2020. Occurrence and weathering of petroleum hydrocarbons deposited on

the shoreline of the North Saskatchewan River from the 2016 Husky oil spill. Environ. Pollut. 258, 113769.